Open

Therapeutic targeting of Chk1 in NSCLC stem cells during chemotherapy

M Bartucci[1], S Svensson[2], P Romania[1], R Dattilo[1], M Patrizii[1], M Signore[1], S Navarra[1], F Lotti[1], M Biffoni[1], E Pilozzi[3], E Duranti[3], S Martinelli[1], C Rinaldo[4], A Zeuner[1], M Maugeri-Saccà[1], A Eramo[1] and R De Maria*[,1,2]

Cancer stem cell (SC) chemoresistance may be responsible for the poor clinical outcome of non-small-cell lung cancer (NSCLC) patients. In order to identify the molecular events that contribute to NSCLC chemoresistance, we investigated the DNA damage response in SCs derived from NSCLC patients. We found that after exposure to chemotherapeutic drugs NSCLC-SCs undergo cell cycle arrest, thus allowing DNA damage repair and subsequent cell survival. Activation of the DNA damage checkpoint protein kinase (Chk) 1 was the earliest and most significant event detected in NSCLC-SCs treated with chemotherapy, independently of their p53 status. In contrast, a weak Chk1 activation was found in differentiated NSCLC cells, corresponding to an increased sensitivity to chemotherapeutic drugs as compared with their undifferentiated counterparts. The use of Chk1 inhibitors in combination with chemotherapy dramatically reduced NSCLC-SC survival *in vitro* by inducing premature cell cycle progression and mitotic catastrophe. Consistently, the co-administration of the Chk1 inhibitor AZD7762 and chemotherapy abrogated tumor growth *in vivo,* whereas chemotherapy alone was scarcely effective. Such increased efficacy in the combined use of Chk1 inhibitors and chemotherapy was associated with a significant reduction of NSCLC-SCs in mouse xenografts. Taken together, these observations support the clinical evaluation of Chk1 inhibitors in combination with chemotherapy for a more effective treatment of NSCLC.
Cell Death and Differentiation (2012) **19,** 768–778; doi:10.1038/cdd.2011.170; published online 25 November 2011

In spite of the large number of clinical trials aimed at improving patient survival, lung cancer is the most common cause of cancer-related mortality worldwide.[1] Based on histology, more than 80% of lung tumors are non-small-cell lung cancers (NSCLCs), whose major subtypes are adenocarcinoma, squamous and large cell carcinomas.[2,3] Recent data indicate that stem cells (SCs) situated throughout the airways may initiate cancer formation and be responsible for the failure of current treatments on lung cancer.[4–6] This concept has changed the view of cancer treatment opening a range of novel therapeutic interventions to prevent tumor recurrence and achieve long-term remission and survival of cancer patients. Cancer SCs (CSCs) are slow-dividing cells that have an unlimited proliferative potential. Several mechanisms have been proposed to explain CSC resistance to conventional therapies, including high expression of anti-apoptotic or multidrug resistance proteins [7–12] and efficient DNA repair system.[13] Such resistance seems to be responsible for tumor relapse or recurrence.[4] Thus, sensitization of CSCs to chemotherapy appears as a major goal toward the improvement of the clinical outcome of patients with incurable tumors.

One of the main hallmarks of neoplastic transformation is deregulation of cell cycle. When defects in cell division are

detected, the DNA damage response prevents phase transition through the activation of cell cycle checkpoints, which induce cell cycle arrest allowing repair of damaged DNA. Critical molecules in the DNA damage machinery after chemotherapy or ionizing radiations (IR) are p53 and the checkpoint protein kinases (Chk) 1 and Chk2. In particular, p53 induces growth arrest by holding the cell cycle at both the G_1/S and G_2/M regulation points,[14,15] whereas Chk1 contributes to DNA damage repair by affecting S-phase and G_2/M phase arrest.[16,17] Unlike Chk2, which is thought to be only an amplifier of checkpoint responses,[18] Chk1 possesses an essential role in the maintenance of DNA integrity. In the event of cell cycle alteration due to DNA damage, Chk1 phosphorylates the family of Cdc25 phosphatases, which in turn inhibit the regulatory protein Cdc2 by preventing its premature activation.[16] As a consequence, cells are arrested at checkpoints until damaged DNA has been repaired. Cdc2 activity depends on the interaction with a co-factor, cyclin B1. Only when dephosphorylated, Cdc2 forms a complex with cyclin B1 and allows dividing cells to enter mitosis from G_2 phase, thus maintaining the highly regulated temporal order of cell cycle progression.[19]

Here, we investigated the mechanisms responsible for NSCLC-SC chemoresistance. We demonstrated that,

---

Table 1 Mutation status of NSCLC-SCs used in this study

	KRAS exon 1	KRAS exon 2	p53 exon 5	p53 exon 6	p53 exon 7	p53 exon 8	EGFR exon 18	EGFR exon 19	EGFR exon 21
NSCLC-SC # 1	WT	WT	WT	**Tyr220Cys, hom.**	WT	WT	WT	WT	WT
NSCLC-SC # 2	WT	WT	WT	**Tyr220Cys, hom.**	WT	WT	WT	WT	WT
NSCLC-SC # 3	WT	WT	WT	WT	WT	WT	WT	WT	WT
NSCLC-SC # 4	WT	WT	WT	WT	**Gly245Cys, hom.**	WT	WT	WT	WT
NSCLC-SC # 5	WT	WT	WT	**Tyr220Cys, hom.**	WT	WT	WT	WT	WT

independently of p53 status, Chk1 activation has a major role in the DNA damage response of NSCLC-SCs and may represent a key therapeutic target for NSCLC.

Results

NSCLC-SCs proficiently repair chemo-induced DNA damage. NSCLC-SCs are undifferentiated and highly clonogenic cells that are largely resistant *in vitro* and *in vivo* to conventional chemotherapy.[4,5] We have previously determined that lung cancer spheres contain a significant percentage of stem-like cells endowed with the ability to self-renew.[5] By limiting dilution analysis such number is higher if compared with freshly dissociated tumor samples and remains stable after serial passages in secondary and tertiary culture (Supplementary Figure S1A). To determine the basis of chemoresistance in NSCLC, we investigated the effects of chemotherapeutic drugs on primary cultures of NSCLC-SCs derived from five different NSCLC patients before and after serum-induced differentiation (Supplementary Figure S1B). All five NSCLC-SC lines were genetically characterized for the presence of common alterations exhibited by lung tumors (Table 1). Cisplatin, gemcitabine and paclitaxel were used at doses comparable with the plasma levels reached in treated lung cancer patients. Unlike in their differentiated progeny, neither of the drugs induced remarkable cell death in NSCLC-SCs even after a long exposure (Figure 1a). Following chemotherapy treatment, NSCLC-SCs underwent a transient growth arrest that lasted until drug removal (Figure 1b). Accordingly, the analysis of cell cycle profile after drug treatment in both p53 wild type (wt) and mutated cells revealed an accumulation of NSCLC-SCs at S and G_2 phase (Figure 1c and Supplementary Figure S2). Specifically, the number of cells in G_2/M increased significantly after cisplatin and paclitaxel treatment, whereas gemcitabine caused a significant accumulation in S phase. Cell cycle arrest may follow DNA damage and checkpoint activation. One of the earliest modifications of the chromatin structure in the damage response is phosphorylation of histone H2A.X at Ser 139 (γ-H2A.X).[20] Short exposure (6 h) of NSCLC-SCs to cisplatin, gemcitabine or paclitaxel resulted in a considerable increase in γ-H2A.X (Figure 1d). However, the persistence of γ-H2A.X was not detectable or only slightly evident after 96 h (Figure 1d), suggesting that NSCLC-SCs are able to efficiently repair the DNA damage induced by chemotherapy. In contrast, the small fraction of differentiated cells that survived 96 h treatment displayed a severely damaged DNA (Supplementary Figure S3A).

NSCLC-SCs resistance to chemotherapy is associated with rapid and sustained Chk1 activation regardless their p53 status. Cell cycle checkpoints are controlled by the ataxia telangiectasia mutated (ATM) and ataxia telangiectasia and Rad3-related protein (ATR) sensor kinases,[21] which phosphorylate downstream effector proteins, such as Chk1 and Chk2.[22,23] Short treatment (6 h) of NSCLC-SCs with either cisplatin, gemcitabine or paclitaxel, promptly induced phosphorylation of ATM (Figure 2a), followed by a strong activation of Chk1 but not Chk2 (Figure 2a), which appears phosphorylated at later time and only after cisplatin and gemcitabine treatment in both p53 wild type and mutated cells (Supplementary Figure S3B right and left panel). Unexpectedly, in p53 wt NSCLC-SC # 3, p53 activation was detectable only as a secondary event in response to DNA damage (Supplementary Figure S3C). These data indicate that chemotherapy-induced DNA damage results in cell cycle arrest mediated mainly by Chk1 and later involving Chk2 and p53. We next compared the activation of Chk1 between NSCLC-SCs and differentiated progeny in both p53-mutated and p53-proficient cells. Interestingly, in both cell types, Chk1 phosphorylation in NSCLC-SCs appeared much higher than in their differentiated counterparts (Figure 2b), suggesting that NSCLC-SCs can more efficiently counteract DNA damage through Chk1 and Chk2 activation independently from their p53 status.

We therefore investigated whether checkpoint abrogation with the specific Chk1/Chk2 inhibitors SB218078[24] and AZD7762 [25] could increase the cytotoxicity of DNA-damaging agents in NSCLC-SCs. Both inhibitors showed a high efficacy in abrogating Chk1-mediated phosphorylation of Cdc25 (Figure 2c). Combination of chemotherapeutic drugs with either of the Chk1 inhibitors prevented DNA repair, as shown by the persistence of γ-H2A.X after 96 h of treatment (Figure 2d and Supplementary Figure S3D), suggesting that in the presence of Chk1 inhibitors NSCLC-SCs lose the ability to repair damaged DNA and may be targeted more efficiently. Accordingly, while having little activity as single agents, Chk1 inhibitors significantly potentiated the cytotoxic effects of gemcitabine, cisplatin and paclitaxel (Figure 2e). Differentiated progenies died after long exposure to chemotherapy independently from the presence of the Chk1 inhibitors (data not shown), confirming that DNA repair activity is much more efficient in NSCLC-SCs as compared with differentiated cells.

To generalize our findings beyond the setting of established NSCLC-SC cell lines, we evaluated the colony-forming ability of freshly dissociated NSCLC cells in the presence of chemotherapy alone or in combination with AZD7762. We found a marked inhibition of sphere formation by the
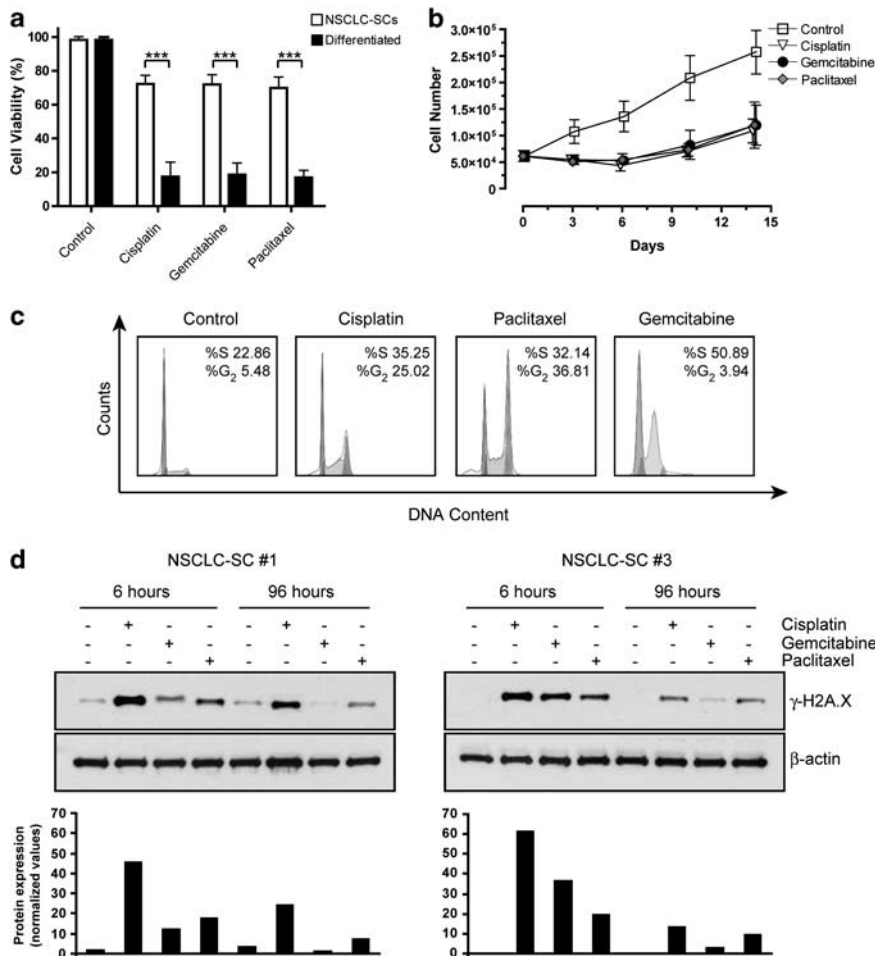
Figure 1 NSCLC-SCs are resistant to conventional chemotherapeutic drugs and efficiently repair DNA damage. (**a**) NSCLC-SCs from five different patients and corresponding differentiated progeny treated with chemotherapeutic drugs for 96 h. Cell viability was measured by CellTiter-Glo assay. The results shown are the mean ± S.D. of three independent experiments.(**b**) Proliferation of untreated NSCLC-SCs (control) or NSCLC-SCs exposed to chemotherapy for 6 days. Data plotted are the results ± S.D. of three independent experiments performed on four different NSCLC-SC lines.(**c**) Representative cell cycle profiles of control or treated NSCLC-SCs. (**d**) γ-H2A.X expression after 6 h and 96 h drugs treatment. β-actin was used as loading control. Lower panels indicate actin-normalized and γ-H2A.X levels for each condition. A representative of three independent experiments is shown. All experiments were performed using 5 μg/ml cisplatin, 50 μM gemcitabine and 30 ng/ml paclitaxel. ***P-value < 0.001

combination of chemotherapy and the Chk1 inhibitor (Figure 2f), thus confirming a preferential targeting of the clonally expanding cells.

Chk1 inhibitors induce mitotic catastrophe through premature activation of Cdc2/cyclin B1 complex in NSCLC-SCs. To gain insight into the molecular mechanisms responsible for increased DNA damage and cell death with the combination of chemotherapeutic drugs and Chk1 inhibitors, we analyzed the expression of Cdc2 and cyclin B1, two cell cycle regulatory proteins known to be controlled by Chk1. We found that inhibition of Chk1 following chemotherapy-induced upregulation of Cdc2 activity by dephosphorylation and decreased expression of cyclin B1 (Figure 3a), probably through nuclear translocation and subsequent degradation. These events lead to abrogation of cell cycle arrest and aberrant mitotic entry before the completion of DNA repair. Cyclin B1 accumulates in the cytoplasm throughout S and G_2 phases and translocates to

the nucleus during prophase.[26] We observed that after 48 h of cisplatin treatment, cyclin B1 was prevalently located in the cytoplasm of NSCLC-SCs, as a sign of cell cycle arrest. By contrast, in cells treated with both cisplatin and SB218078, cyclin B1 translocated from the cytoplasm to the nucleus and forced cells to proceed through the cell cycle (Figure 3b).

The cytotoxic potential of DNA-damaging agents depends on their ability to induce growth arrest and activate the cell death machinery. Cell death can be classified according to enzymological criteria or morphological appearance in apoptosis, necrosis, autophagy or mitotic catastrophe.[27,28] The combination of Chk1 inhibitors and chemotherapeutic drugs induced the formation of a large number of multinucleated NSCLC-SCs (Figures 3c and d), suggesting that cells were dying by mitotic catastrophe.

Treatment with chemotherapeutic drugs and Chk1 inhibitors impairs colony formation of NSCLC-SCs. To investigate the long-term impact of the treatment with
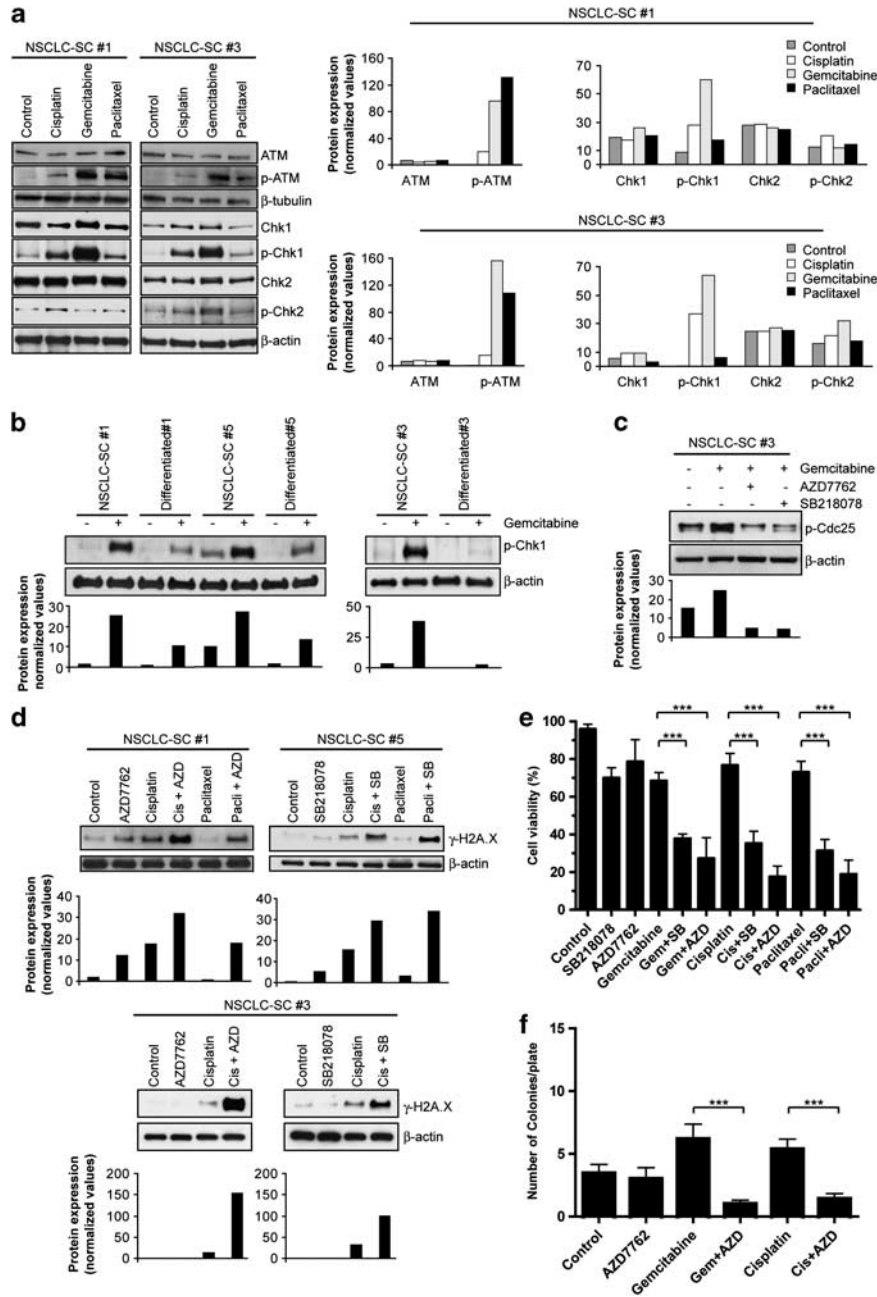
Figure 2 Increased cytotoxicity of chemotherapy by Chk1 inhibitors on NSCLC-SCs. (**a**) Activation of DNA damage proteins in untreated (control) or 6 h treated NSCLC-SC # 1 and NSCLC-SC # 3. (**b**) Western blot analysis for p-Chk1 in NSCLC-SC # 1, NSCLC-SC # 5, NSCLC-SC # 3 and differentiated progenies untreated or treated with gemcitabine for 12 h. (**c**) Modulation of phosphorylated Cdc25C (p-Cdc25) in 24-h-treated NSCLC-SC # 3. (**d**) γ-H2A.X expression in NSCLC-SC # 1, NSCLC-SC # 5 and NSCLC-SC # 3 treated for 96 h as indicated. In each Western blot analysis, the relative densitometric values are normalized over β-tubulin or β-actin. A representative of three independent experiments is shown. (**e**) Cell viability of NSCLC-SCs after treatment with chemotherapy alone or in combination with Chk1 inhibitors. Mean $\pm$ S.D. from four independent experiments performed on five different NSCLC-SC lines is shown. Cells were exposed to 5 μg/ml cisplatin, 50 μM gemcitabine, 30 ng/ml paclitaxel, 20 nM SB218078 and 5 nM AZD7762, respectively. (**f**) Colony-forming ability assay on freshly isolated tumor cells. Mean $\pm$ S.D. of 24 wells/condition obtained by treating and plating cells from four different NSCLC patients. ***P-value < 0.001

anti-neoplastic drugs in combination with Chk1 inhibitors, we performed soft agar assays to evaluate differences in colony-forming abilities. Our results showed that NSCLC-SCs maintain the ability to form colonies after single treatment with cisplatin, paclitaxel or Chk1 inhibitors but not after the combinations of both chemotherapy and SB218078 or AZD7762 (Figures 4a and b). Together these

results confirm that the combination of chemotherapy with Chk1 inhibitors impairs survival and clonogenic activity of NSCLC-SCs.

Chk1 inhibitors potentiate the effect of chemotherapy in NSCLC-SC-based tumor xenografts. Xenotransplantation of tumor SCs may provide a solid preclinical model for the
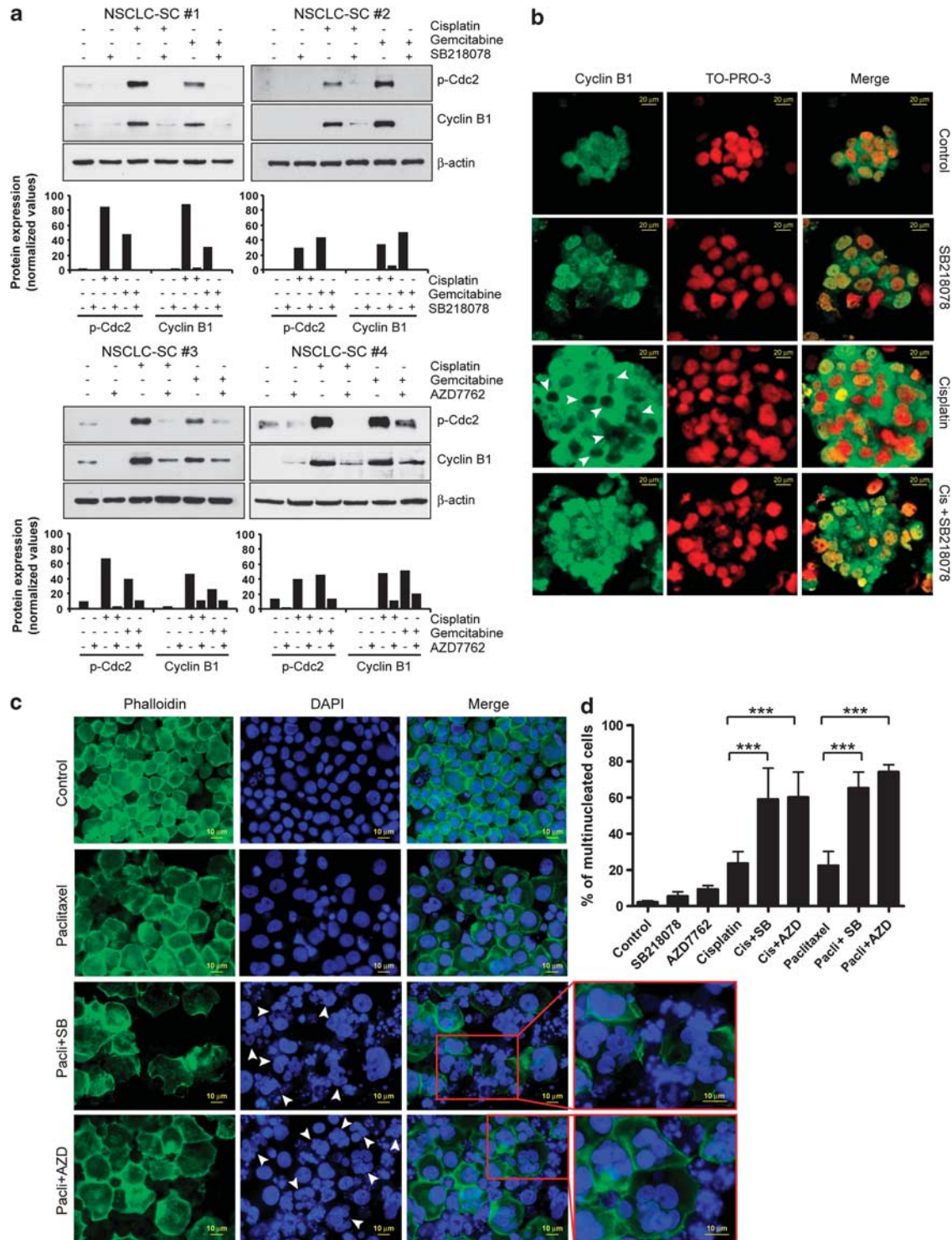
Figure 3 Chk1 inhibition induces Cdc2 activation and mitotic catastrophe in NSCLC-SCs. (**a**) NSCLC-SC # 1, NSCLC-SC # 2, NSCLC-SC # 3 and NSCLC-SC # 4 analyzed for p-Cdc2 and cyclin B1 expression after 96 h of indicated treatments. β-actin was used to assess equal loading. Lower panels indicate actin-normalized protein level for each condition. A representative of three independent experiments is shown. (**b**) Representative immunofluorescence staining for cyclin B1 localization in NSCLC-SCs after 48 h of treatments. Arrowheads indicate cytoplasmic cyclin B1 localization. Acquisition was made with a 40 × objective. (**c**) Representative immunofluorescence of NSCLC-SCs stained with Phalloidin and DAPI to visualize multinucleated cells. Acquisition was made with a 20 × objective. (**d**) Percentage of multinucleated cells estimated by counting nuclei in 100 cells on each Phalloidin-DAPI-stained slide. Arrowheads point to multinucleated cells. Mean ± S.D. of three independent experiments performed on four different NSCLC-SC lines is reported. All experiments were performed with 5 μg/ml cisplatin, 50 μM gemcitabine, 30 ng/ml paclitaxel, 20 nM SB218078 and 5 nM AZD7762. ***P-value < 0.001
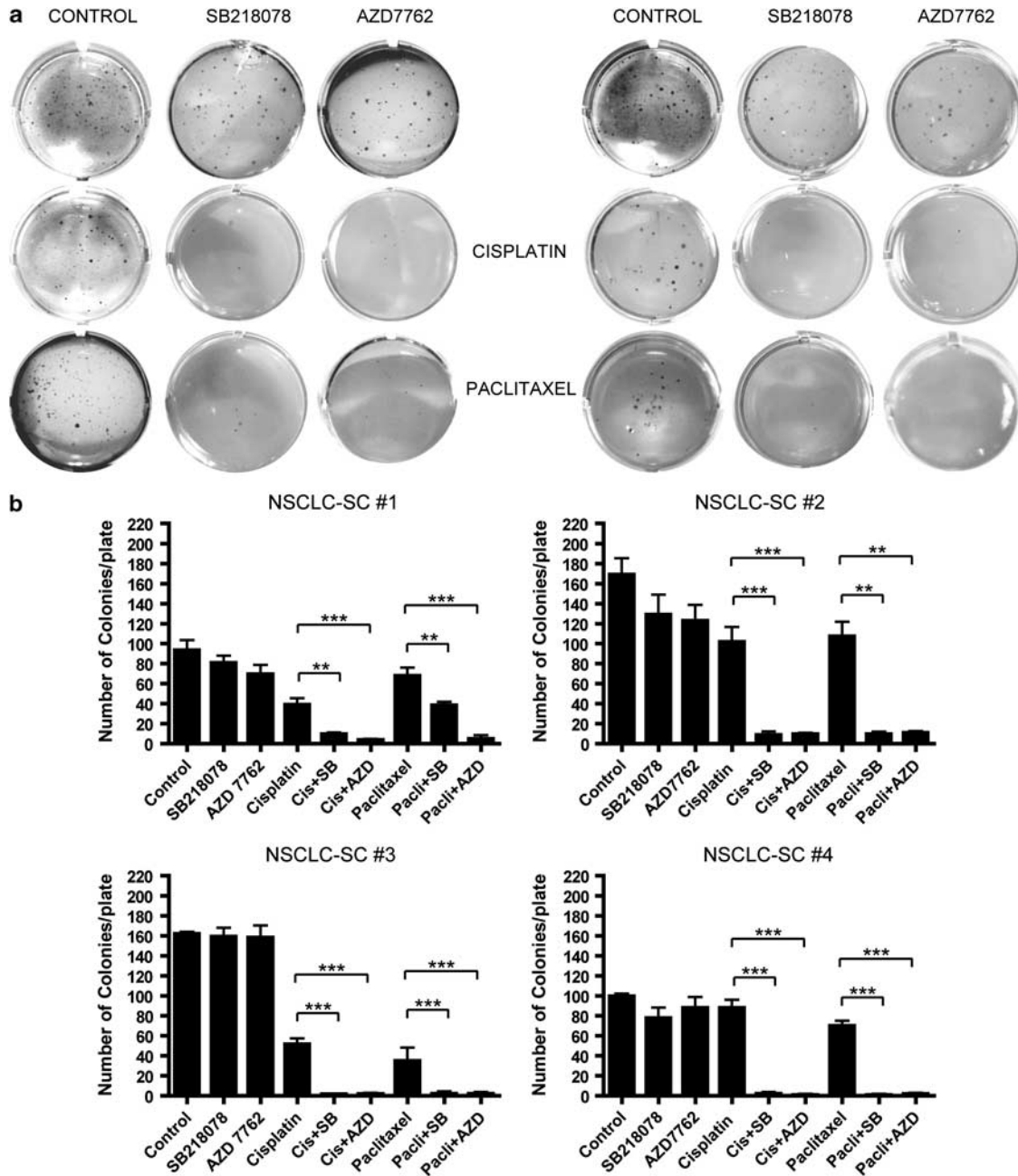
Figure 4 Chk1 inhibition reduces colony-forming ability of NSCLC-SCs. (a) Representative pictures of NSCLC-SC # 1 (left panel) and NSCLC-SC#3 (right panel) colonies obtained in soft agar assay under standard growth condition (control) or after treatment with cisplatin (5 μg/ml) and paclitaxel (30 ng/ml) alone or in combination with SB218078 (20 nM) and AZD7762 (5 nM). (b) Average number of colonies/plate for each indicated condition in NSCLC-SC # 1, NSCLC-SC # 2, NSCLC-SC # 3 and NSCLC-SC # 4. Mean ± S.D. of three independent experiments is shown. **P-value < 0.01, ***P-value < 0.001

development of effective anti-cancer therapies.[29] To evaluate the ability of Chk1 inhibitors to enhance cytotoxicity of anti-neoplastic agents in lung cancer treatment in vivo, we assessed the effect of AZD7762 on human lung carcinoma xenografts generated by subcutaneous transplantation of NSCLC-SCs into NOD-SCID mice, which produce a phenocopy of the original tumor (Figure 5a left and right panel) with a considerably higher efficiency than bulk tumor cells (Supplementary Figure S4). Tumors were allowed to grow until they

reached a size of ~0.3 cm³. Mice were then treated intraperitoneally every 3 days for 4 weeks with chemotherapy alone or in combination with AZD7762, injected intravenously 8 h after chemotherapy. We observed that co-treatment of AZD7762 with gemcitabine or cisplatin significantly affected tumor size (Figure 5b left and right panel) and weight (Figure 5c left and right panel). Because after chemotherapy withdrawal tumors often regrow, a cohort of animals were observed for an extended period of 3 weeks after the last treatment, for a total of
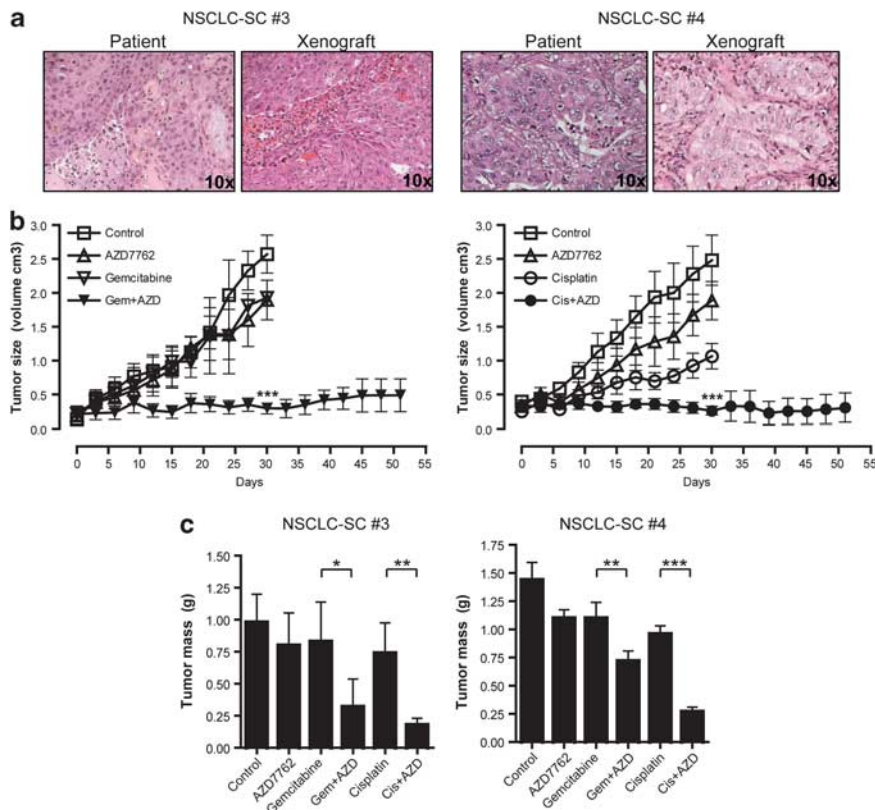
Figure 5 Combination of chemotherapy and Chk1 inhibitors strongly affects tumor growth *in vivo*. (**a**) Hematoxylin and Eosin (H&E) staining of parental tumor (patient) and mouse xenograft from NSCLC-SC # 3 and NSCLC-SC # 4. Acquisition was made with a 10 × objective. (**b**) Growth rate of mouse xenografts generated after subcutaneous injection of NSCLC-SC # 3. Results are mean ± S.D. of four independent experiments. Statistical significance at day 30 was tested by means of two-way repeated measures ANOVA with Bonferroni post-tests (cisplatin *versus* cisplatin + AZD7762 and gemcitabine *versus* gemcitabine + AZD7762). (**c**) Tumor mass for NSCLC-SC # 3 and NSCLC-SC # 4 xenografts measured on day 30. Mean ± S.D. of three experiments is reported. Five mice for each group were treated with gemcitabine (60 mg/kg), cisplatin (3 mg/kg) and AZD7762 (10 mg/kg), as indicated, every 3 days from day 0 to day 27. *P-value < 0.05, **$P < 0.01$, ***$P < 0.001$

51 days post-tumor cells implantation. At the end of the study, changes in tumor size were not significantly appreciable (Figure 5b left and right panel), suggesting that the anti-tumor effects can be protracted after discontinuation of therapy.

The combined treatment with chemotherapy and AZD7762 prevents tumor growth by targeting NSCLC-SCs. We next analyzed the type of damage induced by the different therapeutic regimens on the tumor tissue. Immunohistochemistry and immunofluorescence analysis of tumor xenografts explanted at the end of the treatment showed that only the combination of chemotherapy and AZD7762 was able to kill extensively tumor cells as indicated by the increased expression of γ-H2A.X and the massive presence of deoxyuridine triphosphate nick-end labeling (TUNEL) positive cells, which appeared significantly lower after the treatment with chemotherapy alone (Figures 6a and b upper and lower panel, Supplementary Figure S5A and S5B). Such severe tissue damage was still present 3 weeks after the last delivery of chemotherapy and Chk1 inhibitors, as indicated by the large necrotic areas and rare cellularity observed in the tumors (Figure 6c left and right panel and Supplementary Figure S5C). Thus, the therapeutic response of chemotherapy and Chk1 inhibitors may be extended after discontinuation of the treatment.

To investigate whether the combined treatment with chemotherapy and AZD7762 was able to target NSCLC-SCs *in vivo*, we performed a colony-forming assay on cells derived from dissociation of tumor xenografts, based on the assumption that the number of clonogenic cells should parallel the relative number of tumorigenic cells in treated lesions. We found a significant reduction in the clonogenic ability of cells derived from co-treated xenografts (Figure 6d, right panel), whose human origin was proven by HLA staining (Figure 6d, left panel), confirming that the co-administration of chemotherapeutic drugs and Chk1 inhibitors significantly affects the survival of NSCLC-SCs.

Discussion

The maintenance of genomic stability in normal SCs is essential to preserve the integrity of cell lineages. Efficient DNA damage repair and cell cycle control can be maintained in SCs after oncogenic transformation, as indicated by glioblastoma SC resistance to IR.[13] Here, we show that NSCLC-SCs are considerably more resistant to chemotherapeutic drugs than their differentiated progeny. During exposure to chemotherapy, NSCLC-SCs undergo a growth arrest process readily reversible upon drug removal. In the clinical setting, this behavior could be associated with tumor
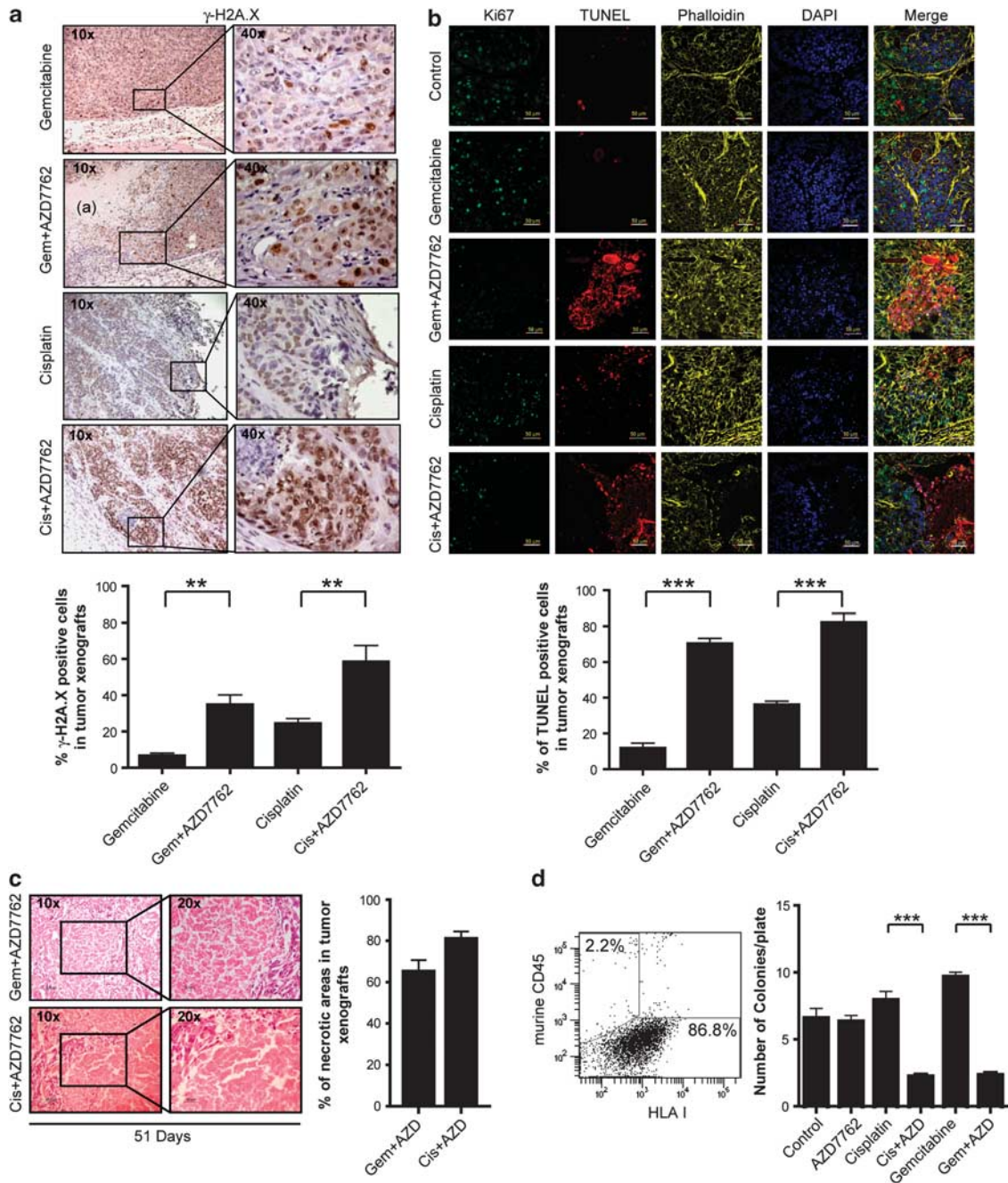
Figure 6 DNA damage, cell death detection and evaluation of clonally expanding NSCLC-SCs in tumor xenografts. (**a**) Representative immunohistochemistry performed on formalin-fixed paraffin-embedded tissue for γ-H2A.X, indicating an extensive necrotic area at day 30. Acquisitions were made with a 10 × and a 40 × objective on NSCLC-SC # 3 xenografts. Lower panel shows the percentage of γ-H2A.X-positive cells in NSCLC-SC # 3 and NSCLC-SC # 4 xenografts. (**b**) Representative Ki67 (green), Phalloidin (yellow) and TUNEL (red) triple staining acquired with a 40 × objective on NSCLC-SC # 3 xenografts sections at day 30. Lower panel shows the percentage of TUNEL positive cells assessed in three independent experiments performed on NSCLC-SC # 3 and NSCLC-SC # 4 xenografts. (**c**) Representative H&E performed on frozen tissue 3 weeks after treatment withdrawal (day 51). Data are representative of three independent experiments performed on mouse xenografts generated after subcutaneous injection of NSCLC-SC # 3. Right panel shows the percentage of necrotic areas in tumor xenografts of both NSCLC-SC # 3 and NSCLC-SC # 4. Acquisitions were made, respectively, with a 10 × and a 20 × objective. (**d**) Flow cytometry analysis for HLA I and colony-forming ability assay performed on tumor cells obtained from dissociation of NSCLC-SC # 3 and NSCLC-SC # 4 xenografts (left panel). Average number of colonies/plate for each combination of treatments (right panel). Mean ± S.D. of two independent experiments with 12 wells/condition is reported. **$P < 0.01$, ***$P < 0.001$

recurrence observed in NSCLC patients treated with chemotherapy, whose survival is extremely poor. The analysis of the molecular mechanisms involved in such chemoresistance showed that upon DNA damage NSCLC-SCs undergo cell cycle arrest preferentially in S or G_2/M phases, thus allowing DNA repair and successful cell duplication. The checkpoint kinase Chk1 has a major role in the DNA damage response and acts as a key regulator of genomic integrity.[30] For this

reason Chk1 represents a critical therapeutic target for cancer treatment.[22,23,31–34] Our results show that Chk1 activation is essential for drug resistance in NSCLC-SCs. Treatment of NSCLC-SCs with gemcitabine, cisplatin or paclitaxel results in a strong activation of Chk1, considerably higher than in differentiated non-tumorigenic cells, indicating that the DNA damage machinery is more robust in NSCLC-SCs than in their progeny.

In human cancers, the high p53 mutation rates result in reliance on S and G_2 checkpoints, controlled by Chk1 and Chk2, to repair DNA damage and promote cell survival. We observed that Chk1 activation is an early response to DNA damage even in p53-wild type NSCLC-SCs. After chemotherapy treatment in NSCLC-SCs, Chk2 phosphorylation and p53 activation in p53 proficient cells occurred days after Chk1 activation, suggesting that Chk1 acts as a major DNA damage checkpoint in NSCLC-SCs, regardless of the p53 status. Accordingly, we observed that Chk1 inhibitors sensitize NSCLC-SCs to chemotherapy by altering the DNA damage response and favoring the incidence of aberrant endomitosis with subsequent cell death. Our results indicate that the Chk1-Cdc25-Cdc2-cyclin B1 pathway is efficiently triggered after drug-induced DNA damage in NSCLC-SCs, as demonstrated by the ability of Chk1 inhibitors to reduce Cdc25 and Cdc2 phosphorylation and promote cyclin B1 translocation to the nucleus.

AZD7762 is a new inhibitor of Chk1 and Chk2, currently in phase I clinical trial in combination with chemotherapy. This drug has been shown to enhance the response to chemotherapy and radiotherapy in preclinical models of colorectal, lung and pancreatic cancer.[25,35,36] Unlike cancer cell lines, CSCs produce tumor xenografts that recapitulate the original tumors and appear a promising tool to study human tumors and devise more effective therapies.[29] Using NSCLC xenografts generated by CSCs, we found that AZD7762 increases considerably the anti-tumor effect of chemotherapy.

Compelling evidence indicates tumor regrowth in NSCLC patients following chemotherapy withdrawal.[37–39] We found that the interruption of co-treatment did not correspond to a rapid rebound in tumor growth, suggesting that co-administration of the Chk1 inhibitor AZD7762 and either gemcitabine or cisplatin could be exploited to devise more effective therapeutic approaches for NSCLC. Moreover, the significant reduction in the number of clonogenic cells in tumor xenografts treated with the combined therapy suggests that such treatment affects the survival of NSCLC-SCs, which are largely spared by chemotherapy alone.

In conclusion, here we show for the first time that primary NSCLC-SCs survive during the course of chemotherapy by exploiting an efficient DNA damage response, which can be prevented by the use of drugs that target Chk1. This distinctive property, which was not found in differentiated NSCLC cells, may explain the inefficacy of chemotherapy in eradicating lung cancer and the consequent poor clinical outcome of NSCLC patients. Inhibition of Chk1 sensitized CSCs to chemotherapy-induced DNA damage and dramatically reduced their survival *in vitro* and *in vivo*. Together our results suggest the hypothesis that Chk1 inhibition might improve the progression-free survival of NSCLC patients during chemotherapy treatment. Due to the number of Chk1 inhibitors currently undergoing early clinical trials, these observations argue in favor of a future clinical evaluation of Chk1 inhibitors in combination with chemotherapy as a cancer-SC-directed therapy, whereas providing substantial preclinical support for future phase II clinical trials with the combination of chemotherapy and Chk1 inhibitors for the treatment of NSCLC.

Materials and Methods

Cell cultures. Lung cancer specimens were obtained upon informed consent from patients undergoing surgical resection according to the Institutional Ethical Committee guidelines on human experimentation and with the Helsinki Declaration. NSCLC-SCs and differentiated progenies from human adenocarcinoma (NSCLC-SC # 1 and NSCLC-SC # 4), human squamous cell carcinoma (NSCLC-SC # 2 and NSCLC-SC # 3) and human large cell neuroendocrine carcinoma (NSCLC-SC # 5), were obtained from patients who underwent surgical resection of lung tumors and cultured as previously described.[5] Briefly, surgical specimens dissociation was carried out by enzymatic digestion (20 mg/ml collagenase II, Gibco-Invitrogen, Carlsbad, CA, USA) for 2 h at 37 °C. Recovered cells were cultured at clonal density in serum-free medium supplemented with 20 mg/ml epidermal growth factor (EGF) and 10 mg/ml basic fibroblast growth factor (b-FGF). Flasks non-treated for tissue culture were used to reduce cell adherence and support growth as undifferentiated tumor spheres. The medium was replaced or supplemented with fresh growth factors twice a week until cells started to grow forming floating aggregates. Cultures were expanded by mechanical dissociation of spheres, followed by re-plating of both single cells and residual small aggregates in complete fresh medium. To obtain differentiation of lung cancer sphere-forming cells, stem cell medium was replaced for 3 days with Bronchial Epithelial Cell Growth Medium (Cambrex, East Rutherford, NJ, USA) in tissue culture-treated flasks, to allow cell attachment and differentiation. Adherent cells were thereafter grown in DMEM supplemented with 10% serum. The acquisition of differentiation markers was evaluated by immunofluorescence.

Molecular analysis. Mutational screening was performed on the coding exons 1 and 2 of *KRAS*, exons 5 to 8 of *TP53* and the *EGFR* cDNA portion coding for the *N*-terminal region of the tyrosine kinase domain (residues 711–863). Genomic DNA specimens were obtained from NSCLC-SCs using PureLinkTM Genomic DNA Purification Kit (Invitrogen, Carlsbad, CA, USA) according to the manufacturer's protocols. Total RNA was extracted from NSCLC-SCs using the RNeasy mini kit (Qiagen, Hilden, Germany). RNA (1 μg) was reverse transcribed into cDNA by using SuperScript II RT with oligo(dT) as primers (Invitrogen) according to the manufacturer's protocol. PCR amplifications were carried out using high-fidelity Optimase polymerase (Transgenomic, Omaha, NE, USA). Primer pairs and PCR conditions are listed in Supplementary Methods Table 1. Unpurified PCR products were analyzed by denaturing high-performance liquid chromatography (DHPLC) with the Wave 2100 DNA fragment analysis system (Transgenomic) at column temperatures recommended by Navigator software, version 1.6.4.12 (Transgenomic). Heterozygous templates with previously identified mutations or single nucleotide polymorphisms were used as positive controls in each DHPLC run. DHPLC analysis of pooled DNAs was performed to explore possible occurrence of homozygous/hemizygous condition for mutations. Amplimers with abnormal denaturing profiles were re-amplified, purified (Microcon PCR; Millipore, Bedford, MA, USA) and sequenced bidirectionally using the ABI BigDye Terminator Sequencing Kit v.1.1 (Applied Biosystems, Carlsbad, CA, USA) and an ABI Prism 310 Genetic Analyzer (Applied Biosystems)**.**

Reagents. Cisplatin was purchased from Teva (Petach Tikva, Israel), gemcitabine from Lilly (Indianapolis, IN, USA), paclitaxel from Sigma-Aldrich (St. Louis, MO, USA), SB218078 from Calbiochem (Nottingham, UK) and AZD7762 from Axon Medchem (Groningen, The Netherlands).

Treatments. For *in vitro* experiments the following compounds were used: cisplatin (5 μg/ml), gemcitabine (50 μM), paclitaxel (30 ng/ml), SB218078 (20 nM) and AZD7762 (5 nM). For *in vivo* studies we used: gemcitabine (60 mg/kg), cisplatin (3 mg/kg) and AZD7762 (10 mg/kg). Chk1 inhibitors were added 8 h after chemotherapy for both *in vitro* and *in vivo* studies.

Cell viability assays. For chemoresistance comparison and cell viability studies, dissociated spheres and adherent differentiated cells were plated in 96 well plates at 5000 cells/well in growth medium supplemented with cisplatin, gemcitabine or paclitaxel, for 96 h. For cell viability studies, dissociated NSCLC-SCs were seeded and treated as described above and in combination with Chk1 inhibitors. Cell viability was evaluated after 96 h by CellTiter-Glo Luminescent Cell Viability Assay (Promega, Madison, WI, USA) according to standard protocols and analyzed with a Victor 2 plate reader (Wallac, Turku, Finland).

Cell proliferation assays. Dissociated NSCLC-SCs were treated with cisplatin, gemcitabine or paclitaxel for 6 days. On day 3 cells were collected, counted by Trypan Blue exclusion and replated in the presence of chemotherapy. On day 6 cells were collected, counted by Trypan Blue exclusion and replated in fresh medium without chemotherapy. Thereafter, cells were counted and replated every 3 days until day 15.

Cell cycle analysis. NSCLC-SCs were dissociated and treated with cisplatin, gemcitabine or paclitaxel. After 48 h, cells were stained with a propidium iodide (PI) staining solution (trisodium citrate 0.1%, NaCl 9.65 mM, NP40 0.3%, PI 50 μg/ml and RNase A 200 μg/ml) for 30 min at RT. Cell cycle profile was acquired with a FACSCanto flow cytometer (Becton Dickinson, Franklin Lakes, NJ, USA) and analyzed with FlowJo software (Tree Star Inc.; http://www.flowjo.com/index.php).

Western blot. NSCLC-SCs were treated for 6 h, 12 h, 24 h or 96 h as previously described. Whole-cell lysates (20 μg) were fractioned on SDS-polyacrylamide gels, blotted to nitrocellulose membranes and incubated with the following antibodies: Chk1, phosphorylated Chk1 (Ser345), Chk2 (1C12), phosphorylated Chk2 (Thr68), phosphorylated Cdc25C (Ser216) and phosphorylated Cdc2 (Tyr15) from Cell Signaling Technology (Danvers, MA, USA); ATM (5C2), phosphorylated ATM (0H11.E12) and cyclin B1 (clone D-11) from Santa Cruz Biotechnology (Santa Cruz, CA, USA); phosphorylated H2A.X (Ser139) (γ-H2A.X) from Upstate-Millipore (Billerica, MA, USA), β-actin (AC-15) and β-tubulin (TUB 2.1) from Sigma-Aldrich, and detected using enhanced chemiluminescence detection kit (Pierce, Rockford, IL, USA). Densitometric analysis was performed using Scion Image (Scion Corporation, Frederick, MO, USA) and all results were normalized over β-actin or β-tubulin (ATM and p-ATM).

Immunofluorescence. Cells were treated with cisplatin, paclitaxel, SB218078 or AZD7762 alone or in combinations for 48 or 96 h. For cyclin B1 staining, treated cells were fixed with 2% paraformaldehyde and then permeabilized with 0.1% Triton X-100/PBS for 1 h at 37 °C before incubation with cyclin B1 (clone D-11, Santa Cruz Biotechnology) overnight at 4 °C. Thereafter, slides were incubated with Alexa Fluor 488 goat anti-mouse (1 μg/ml, Invitrogen) for 1 h at RT. TO-PRO-3 (4 μM, Invitrogen) and Phalloidin-AlexaFluor 488 (5Units/ml, Molecular Probes/Invitrogen) were used to visualize nuclei and F-actin cytoskeleton. For tumor xenografts immunofluorescence, resected tumors were fixed with 10% (vol/vol) formalin (BioOptica, Milan, Italy) for 24 h and subsequently passed from 10% to 30% concentrations of sucrose. Tumors were mounted in Killik frozen section medium (BioOptica) and 5 μm-thick sections were cut and incubated with terminal deoxynucleotidyl transferase-mediated TUNEL reaction mixture (Roche, Basel, Switzerland) for 1 h at RT followed by anti-Ki67 (DAKO, Glostrup, Denmark) overnight at 4 °C. AlexaFluor 555-conjugated goat anti-mouse secondary antibody (1 μg/ml, Invitrogen) was incubated for 1 h at RT. Nuclei and cytoskeleton were counterstained using DAPI and Alexa Fluor 647-conjugated Phalloidin (Invitrogen), respectively. Slides were subsequently mounted using an anti-fade mounting medium (Invitrogen) and analyzed using an Olympus FV-1000 spectral confocal microscope equipped with an UltraPlan Apochromatic 60 × NA 1.35 and an UltraPlan Fluorite 40 × NA 1.3 objectives and the software Olympus Fluoview (Olympus, Tokyo, Japan). To evaluate the percentage of TUNEL positive cells in tumor xenografts, image analysis was performed with ImageJ (http://rsb.info.nih.gov/ij/). Single channels were extracted from the confocal images either for nuclei (DAPI) or for TUNEL (TMR-Red), and after application of a threshold that eliminates background dust, a watershed filter was applied on the binary images. The tool for particle analysis was used to quantify the amount of TUNEL positivity as compared with the number of DAPI-stained nuclei/particles.

Colony-forming ability assay. Soft agar colony-forming assays were carried out for NSCLC-SCs treated with cisplatin or paclitaxel either alone or in combination with SB218078 or AZD7762 for 96 h. Subsequently, cells were washed and 500 single cells were plated in the top agar layer in each well of a 24-well culture plate with 0.3% top agar layer and 0.4% bottom agar layer (SeaPlaque Agarose, Cambrex, NJ, USA). Cultures were incubated at 37 °C for 20 days. Colonies from triplicate wells were stained with crystal violet (0.01% in 10% MetOH), visualized and counted under microscope and photographed. To evaluate the colony-forming ability of freshly isolated cancer cells, human tumors were obtained from four NSCLC patients who underwent surgical resection and dissociated as previously described.[5] In order to eliminate contaminating non-tumoral cells, recovered cells were stained with FITC-conjugated epithelial cell adhesion molecule (EpCAM) (DakoCytomation, Glostrup, Denmark) and sorted with a FACS Aria (Becton Dickinson). Thereafter, cells were treated with gemcitabine and cisplatin alone or in combination with AZD7762 for 96 h, extensively washed and plated at 500 cells/well, using 24 wells for each condition. After 50 days, colonies were stained, visualized and counted under the microscope. To obtain xenograft-derived cells, tumors were aseptically removed and dissociated. Cells recovered were extensively washed, plated in stem cell medium for 4 days and subsequently 500 cells for each treatment condition were plated as described above. After 20 days, colonies were visualized and counted as described above.

In vivo studies. Five-week-old female NOD-SCID mice from Charles River Laboratories (Wilmington, MA, USA) were maintained in accordance with the institutional guidelines of the Istituto Superiore di Sanità Animal Care Committee. NSCLC-SCs were dissociated, counted and resuspended in a mix of PBS and Matrigel (1 : 1). To obtain synchronized tumors in about 4 weeks, 50 000 NSCLC-SCs were injected subcutaneously into the right flank of each mouse. Tumors were allowed to grow to the size of ~ 0.3 cm^3 before the administration of compounds. Mice were treated intraperitoneally with either gemcitabine (60 mg/kg) or cisplatin (3 mg/kg), and intravenously with AZD7762 (10 mg/kg) every 3 days. Tumor growth was evaluated with an electronic caliper before every administration. After 30 days, tumors were removed and weighed using a PL202-L Precision Balance (Mettler-Toledo, Novate Milanese, Italy). To evaluate drugs combination efficacy, tumors were allowed to grow in the absence of treatment and measured every 3 days until day 51. Immunohistochemistry was performed on formalin-fixed paraffin-embedded tissues or frozen tissues. Paraffin sections (5 μm) were dewaxed in xylene and rehydrated with distilled water and subsequently incubated with anti-γ-H2A.X (Upstate-Millipore). The reaction was performed using Elite Vector Stain ABC systems (Vector Laboratories, Burlingame, CA, USA) and DAB substrate chromogen (DakoCytomation), followed by counterstaining with haematoxylin. H&E staining was performed on 5 μm frozen sections and observed through a Nikon Eclipse E1000 transmitted light right microscope equipped with PlanFluor 10 × and 20 × dry objectives (Nikon, Melville, NY, USA). Images were subsequently taken by using a Nikon DXM1200 RGB camera and the Nikon ACT-1 software. Percentage of γ-H2A.X-positive cells in tumor xenografts was assessed by counting five different fields in each slide derived from two independent experiments. Percentage of necrotic areas was evaluated by comparing in each slide the number of pixels included in necrotic *versus* viable areas. Image analysis was performed with ImageJ (http://rsb.info.nih.gov/ij/). Human origin of the tumor xenografts was confirmed by FACS analysis with a PE conjugated anti-HLA class I antibody (eBioscience, San Diego, CA, USA), whereas a PE-Cy5 anti-mouse CD45 antibody (BD Pharmingen, San Diego, CA, USA) was used to exclude unspecific staining of mouse cells.

Statistical analysis. All statistical analyses were performed using GraphPad Prism 4 (GraphPad Software Inc., http://www.graphpad.com/welcome.htm). Data are presented as mean ± standard deviation (S.D.). Statistical significance was determined by ANOVA (one-way or two-way) with Bonferroni post-test. A P value < 0.05 is represented by a single asterisk, a P value < 0.01 is represented by a double asterisk, whereas three asterisks indicate $P < 0.001$.

Conflict of Interest

The authors declare no conflict of interest.

1. Jemal A, Siegel R, Ward E, Hao Y, Xu J, Thun MJ. Cancer statistics, 2009. *CA Cancer J Clin* 2009; **59**: 225–249.
2. Travis WD, Travis LB, Devesa SS. Lung cancer. *Cancer* 1995; **75** (1 Suppl): 191–202.
3. Collins LG, Haines C, Perkel R, Enck RE. Lung cancer: diagnosis and management. *Am Fam Physician* 2007; **75**: 56–63.
4. Bertolini G, Roz L, Perego P, Tortoreto M, Fontanella E, Gatti L *et al*. Highly tumorigenic lung cancer CD133+ cells display stem-like features and are spared by cisplatin treatment. *Proc Natl Acad Sci USA* 2009; **106**: 16281–16286.
5. Eramo A, Lotti F, Sette G, Pilozzi E, Biffoni M, Di Virgilio A *et al*. Identification and expansion of the tumorigenic lung cancer stem cell population. *Cell Death Differ* 2008; **15**: 504–514.
6. Kim CF, Jackson EL, Woolfenden AE, Lawrence S, Babar I, Vogel S *et al*. Identification of bronchioalveolar stem cells in normal lung and lung cancer. *Cell* 2005; **121**: 823–835.
7. Pan CX, Zhu W, Cheng L. Implications of cancer stem cells in the treatment of cancer. *Future Oncol* 2006; **2**: 723–731.
8. Seigel GM, Campbell LM, Narayan M, Gonzalez-Fernandez F. Cancer stem cell characteristics in retinoblastoma. *Mol Vis* 2005; **11**: 729–737.
9. Ho MM, Ng AV, Lam S, Hung JY. Side population in human lung cancer cell lines and tumors is enriched with stem-like cancer cells. *Cancer Res* 2007; **67**: 4827–4833.
10. Shi GM, Xu Y, Fan J, Zhou J, Yang XR, Qiu SJ *et al*. Identification of side population cells in human hepatocellular carcinoma cell lines with stepwise metastatic potentials. *J Cancer Res Clin Oncol* 2008; **134**: 1155–1163.
11. Wang YH, Li F, Luo B, Wang XH, Sun HC, Liu S *et al*. A side population of cells from a human pancreatic carcinoma cell line harbors cancer stem cell characteristics. *Neoplasma* 2009; **56**: 371–378.
12. Dean M, Fojo T, Bates S. Tumour stem cells and drug resistance. *Nat Rev Cancer* 2005; **5**: 275–284.
13. Bao S, Wu Q, McLendon RE, Hao Y, Shi Q, Hjelmeland AB *et al*. Glioma stem cells promote radioresistance by preferential activation of the DNA damage response. *Nature* 2006; **444**: 756–760.
14. Kastan MB, Onyekwere O, Sidransky D, Vogelstein B, Craig RW. Participation of p53 protein in the cellular response to DNA damage. *Cancer Res* 1991; **51** (23 Part 1): 6304–6311.
15. Vogelstein B, Lane D, Levine AJ. Surfing the p53 network. *Nature* 2000; **408**: 307–310.
16. Xiao Z, Chen Z, Gunasekera AH, Sowin TJ, Rosenberg SH, Fesik S *et al*. Chk1 mediates S and G2 arrests through Cdc25A degradation in response to DNA-damaging agents. *J Biol Chem* 2003; **278**: 21767–21773.
17. Chen Z, Xiao Z, Chen J, Ng SC, Sowin T, Sham H *et al*. Human Chk1 expression is dispensable for somatic cell death and critical for sustaining G2 DNA damage checkpoint. *Mol Cancer Ther* 2003; **2**: 543–548.
18. Bartek J, Lukas J. Chk1 and Chk2 kinases in checkpoint control and cancer. *Cancer Cell* 2003; **3**: 421–429.
19. Johnson DG, Walker CL. Cyclins and cell cycle checkpoints. *Annu Rev Pharmacol Toxicol* 1999; **39**: 295–312.
20. Rogakou EP, Pilch DR, Orr AH, Ivanova VS, Bonner WM. DNA double-stranded breaks induce histone H2AX phosphorylation on serine 139. *J Biol Chem* 1998; **273**: 5858–5868.
21. Abraham RT. Cell cycle checkpoint signaling through the ATM and ATR kinases. *Genes Dev* 2001; **15**: 2177–2196.
22. Gatei M, Sloper K, Sorensen C, Syljuasen R, Falck J, Hobson K *et al*. Ataxia-telangiectasia-mutated (ATM) and NBS1-dependent phosphorylation of Chk1 on Ser-317 in response to ionizing radiation. *J Biol Chem* 2003; **278**: 14806–14811.
23. Matsuoka S, Rotman G, Ogawa A, Shiloh Y, Tamai K, Elledge SJ. Ataxia telangiectasia-mutated phosphorylates Chk2 *in vivo* and *in vitro*. *Proc Natl Acad Sci USA* 2000; **97**: 10389–10394.
24. Jackson JR, Gilmartin A, Imburgia C, Winkler JD, Marshall LA, Roshak A. An indolocarbazole inhibitor of human checkpoint kinase (Chk1) abrogates cell cycle arrest caused by DNA damage. *Cancer Res* 2000; **60**: 566–572.
25. Zabludoff SD, Deng C, Grondine MR, Sheehy AM, Ashwell S, Caleb BL *et al*. AZD7762, a novel checkpoint kinase inhibitor, drives checkpoint abrogation and potentiates DNA-targeted therapies. *Mol Cancer Ther* 2008; **7**: 2955–2966.
26. Jin P, Hardy S, Morgan DO. Nuclear localization of cyclin B1 controls mitotic entry after DNA damage. *J Cell Biol* 1998; **141**: 875–885.
27. Melino G. The Sirens' song. *Nature* 2001; **412**: 23.
28. de Bruin EC, Medema JP. Apoptosis and non-apoptotic deaths in cancer development and treatment response. *Cancer Treat Rev* 2008; **34**: 737–749.
29. Baiocchi M, Biffoni M, Ricci-Vitiani L, Pilozzi E, De Maria R. New models for cancer research: human cancer stem cell xenografts. *Curr Opin Pharmacol* 2010; **10**: 380–384.
30. Cho SH, Toouli CD, Fujii GH, Crain C, Parry D. Chk1 is essential for tumor cell viability following activation of the replication checkpoint. *Cell Cycle* 2005; **4**: 131–139.
31. Merry C, Fu K, Wang J, Yeh IJ, Zhang Y. Targeting the checkpoint kinase Chk1 in cancer therapy. *Cell Cycle* 2010; **9**: 279–283.
32. Ashwell S, Janetka JW, Zabludoff S. Keeping checkpoint kinases in line: new selective inhibitors in clinical trials. *Expert Opin Investig Drugs* 2008; **17**: 1331–1340.
33. Kawabe T. G2 checkpoint abrogators as anticancer drugs. *Mol Cancer Ther* 2004; **3**: 513–519.
34. Bucher N, Britten CD. G2 checkpoint abrogation and checkpoint kinase-1 targeting in the treatment of cancer. *Br J Cancer* 2008; **98**: 523–528.
35. Mitchell JB, Choudhuri R, Fabre K, Sowers AL, Citrin D, Zabludoff SD *et al*. In vitro and *in vivo* radiation sensitization of human tumor cells by a novel checkpoint kinase inhibitor, AZD7762. *Clin Cancer Res* 2010; **16**: 2076–2084.
36. Morgan MA, Parsels LA, Zhao L, Parsels JD, Davis MA, Hassan MC *et al*. Mechanism of radiosensitization by the Chk1/2 inhibitor AZD7762 involves abrogation of the G2 checkpoint and inhibition of homologous recombinational DNA repair. *Cancer Res* 2010; **70**: 4972–4981.
37. El Sharouni SY, Kal HB, Battermann JJ. Accelerated regrowth of non-small-cell lung tumours after induction chemotherapy. *Br J Cancer* 2003; **89**: 2184–2189.
38. Lara Jr PN, Redman MW, Kelly K, Edelman MJ, Williamson SK, Crowley JJ *et al*. Disease control rate at 8 weeks predicts clinical benefit in advanced non-small-cell lung cancer: results from Southwest Oncology Group randomized trials. *J Clin Oncol* 2008; **26**: 463–467.
39. Birchard KR, Hoang JK, Herndon Jr JE, Patz Jr EF. Early changes in tumor size in patients treated for advanced stage nonsmall cell lung cancer do not correlate with survival. *Cancer* 2009; **115**: 581–586.